OBSERVATIONS OF NEEDLE FUNCTIONING AND STAND PHENOLOGY IN PERMAFROST-AFFECTED BOREAL FOREST STANDS

Wayne Dawson III[1], Andrew Jablonksi[1], Jennifer Watts[2], Howard Epstein[1], Xi Yang[1]

[1]University of Virginia, [2]Woodwell Climate Research Center

Abstract

Boreal ecosystems are experiencing more rapid climate shifts than lower latitudes due to anthropogenic climate change. These shifts are leading to rising temperatures, strengthened wildfire regimes, and increasing carbon emissions from soils and permafrost, contributing to a positive climate feedback. However, these climate shifts may also lead to increased carbon uptake by altering leaf physiology, increasing growing season length, and altering forest composition. Here, we leverage needle-level PAM fluorometry and tower-based remote sensing metrics to monitor the physiology and phenology of a permafrost affected boreal forest near Fairbanks, Alaska. From the needle-level observations, we find that non-regulated energy dissipation mechanisms give way to photosynthesis during the winter to spring transition, with temperature acting as a major control. From the remote sensing measurements, we find that some vegetation indices, such as the normalized difference vegetation index, primarily respond to snow and ice crystal melting, even when instrument field of view is restricted to exclude the understory background. We also find that solar-induced fluorescence can become noisy due to signal limitations under such a reduced field of view. Future work will concentrate on comparing physiology and remote sensing measurements to environmental conditions to identify potential drivers.

Introduction and Background

Boreal Forests in a Changing Landscape:
Anthropogenic change is altering the world's ecosystems at unprecedented rates by changing historical climate regimes. These changes vary across regions but tend to be most intense at high northern latitudes through a phenomenon called polar amplification.[1] This amplification has contributed to rising surface temperatures, more frequent wildfires, and varied shifts in forest structure and composition.[2-5] The complexity and spatially variable nature of these changes limit our understanding of how boreal forests will respond to future change. However, observational data suggests that the vast amounts of carbon stored in boreal regions will be threatened by increasing carbon emissions.[6]

Increasing boreal carbon emissions are a product of numerous drivers. Increasing wildfire frequency and destabilization of permafrost carbon stores have been linked to significant carbon emissions across the boreal domain.[7] Rising temperatures, meanwhile, can drive carbon emissions by enhancing soil and plant respiration, though recent experimental work suggests acclimation will limit respiratory change.[8] Temperature changes are also leading to increased decomposition of soil carbon by drying waterlogged soils.[9] These shifts towards carbon emission will produce a positive climate feedback without compensating increases in productivity.

Changes in boreal productivity under climate change are highly uncertain due the multiple scales over which change is occurring. At the leaf level, carbon uptake is dependent on acclimation of photosynthetic physiology to new climate and moisture regimes.[10] Increasingly dry conditions like those under climate change have been

observed to limit needle photosynthesis in some species but not others.[11-12] Under stress conditions, downregulation of photosynthesis manifests by redirecting absorbed light energy away from photosynthesis and into non-regulated heat dissipation, non-photochemical quenching – which dissipates the energy through regulated changes in heat emitting pigments like xanthophylls – and fluorescence – which re-emits the energy as light.[13] To develop an integrated understanding of how environmental change alters leaf functioning, in situ observations of this partitioning across seasons and environmental conditions are needed.

At the stand level, carbon uptake is dependent on shifts in species composition, stand level physiology, and the timing, or phenology, of photosynthesis. Due to changes in climate and increases in wildfire intensity, boreal forests are expected to increasingly shift from evergreen to deciduous species.[14] These emerging deciduous stands take up more carbon and maintain larger soil carbon pools than their evergreen counterparts.[15] Furthermore, across both stand types, climatic shifts towards warmer springs are expected to advance timing of snowmelt and photosynthetic onset, leading to longer growing seasons and further increasing carbon uptake.[16] However, longer growing seasons will lead to increased photosynthetic water demands, which may limit potential increases in carbon uptake.[17] In forests underlain by permafrost, melting-driven increases in soil moisture may counteract drying.[18] Ultimately, to understand how boreal carbon dynamics will shift in the future, we must understand how changes in environmental drivers will alter physiology and phenology.

Monitoring of Physiology and Phenology in Boreal Forests: Due to the large extent of boreal forests, our understanding of boreal physiology and phenology is largely derived from small scale, leaf-level measurements and broad scale remote sensing approaches. Measurements of leaf-level physiology are dominated by the pulse-amplitude modulation (PAM) fluorometry technique. During the day, light energy is partitioned between photosynthesis, non-regulated heat dissipation, non-photochemical quenching (NPQ), and chlorophyll fluorescence. NPQ processes function to divert excess light energy away from the photosystem through regulated changes in heat-emitting pigments.[19] Fluorescence, in contrast, involves light energy being re-emitted by chlorophyll in the red to far-red wavelengths.[20] PAM fluorometry techniques utilize rapid laser pulses that saturate the photosynthetic system without altering rates of NPQ.[13] By monitoring fluorescence levels before and during daytime saturation pulses, the amount of light energy being partitioned to photosynthesis can be calculated. Similarly, during the night where reversible NPQ is inactive, saturation pulses can be used to determine the theoretical maximum amount of light partitioned to photosynthesis and the extent of NPQ. Historically, this technique has largely been used in boreal forests to understand how evergreen trees use NPQ to suppress photosynthesis during harsh winter conditions, focusing on light and temperature as potential environmental drivers.[21-22] To better understand how boreal physiology will respond to anthropogenic changes, incorporating environmental factors beyond light and temperature will be necessary, particularly in the permafrost zone where melting may alter local hydrology.

At broader scales, satellite remote sensing efforts have produced conflicting observations of changes in boreal physiology overtime. Satellite observations of vegetation greenness using spectral indices like the normalized difference vegetation index (NDVI) suggest mixed trends of greening and

browning.[23-24] Satellite-based monitoring of phenology through NDVI, meanwhile, has supported predictions of earlier spring photosynthetic onset and increased growing season length.[25] However, the usage of greeness-based metrics like NDVI for assessing plant status is questionable in boreal regions. First, many boreal forests are dominated by evergreen vegetation, for which changes in greenness are more subtle and not as tightly coupled to shifts in photosynthetic activity.[26] Second, these systems experience persistent snow cover and ice crystal formation that adds noise to commonly used spectral indices NDVI.[27] To understand the physiology and phenology of these rapidly changing landscapes, novel techniques that more directly respond to plant functioning and are resilient to snow effects must be used.

Solar-induced fluorescence (SIF) is small radiative signal that can be emitted by chlorophyll following light absorption. Unlike PAM fluorescence, which is laser-stimulated, SIF is passively emitted using solar energy, with it competing with photosynthesis and non-photochemical quenching processes for light energy.[28] Recent technological advances have enabled the small SIF signal to retrieved instruments installed on research towers, planes, and satellites.[29] At coarse spatiotemporal scales, SIF has been well correlated with gross primary production across biomes.[30] At finer scales, SIF is well correlated with GPP for evergreen stands and has been used alongside conventional spectral indices to identify mechanisms underlying photosynthetic phenology.[31] Furthermore, due to it being emitted by vegetation, SIF is more resilient to background effects like snow than vegetation indices.[27] Ultimately, SIF's direct connection to the photosynthetic system makes it ideal for monitoring physiological dynamics in rapidly changing boreal regions.

This research aims to leverage in-situ PAM fluorometry and SIF measurements alongside a suite of environmental data to better understand how natural variations in environmental drivers are linked to shifts in boreal physiology and phenology across spatiotemporal scales and plant types. Our guiding questions are:

1) How does photosynthetic physiology, particularly the partitioning of energy between photosynthesis, non-photochemical quenching, and fluorescence, respond to environmental changes at diurnal, daily, and seasonal timescales?
2) How effectively can snowmelt, greenness, and photosynthetic phenology be captured by remote sensing phenometrics over boreal forest stands?
3) What environmental drivers are most strongly associated with snowmelt phenology, greenness phenology, and photosynthetic phenology in permafrost-affected boreal forests?

Methods

Site Description: Caribou-Poker Creeks Research Watershed (Site Name: BONA) is located in interior Alaska (65.154°N, 147.503°W) and is a terrestrial core site in the National Ecological Observatory Network (NEON). It experiences a mean annual temperature of -3.0°C and a mean annual precipitation of 262mm, around 30% of which is snowfall.[32] Daily average temperatures have increased at the site since 1980, with warm winter days becoming more common. This

warming has contributed to losses in the region's discontinuous permafrost.

BONA consists of a mixture of hardwood forests, shrublands, and wetlands, with species composition responding to local hydrology. In poorly drained lowland areas, shrubs and mosses like dwarf birch (*Betula nana*), bog-labrador tea (*Rhododendron groenlandicum*), and splendid feather moss (*Hycominium splendens*) are common. In wet moderately drained soils, black spruce (*Picea mariana*) forms open evergreen stands. In more well drained and recently disturbed sites, deciduous trees such as Alaskan paper birch (*Betula neoalaskana*) and quaking aspen (*Populus tremuloides*) are common. Within BONA, NEON has installed a 18m research tower overlooking a black spruce stand for hosting eddy-covariance and meteorological instruments (hereafter: black spruce tower). This is complimented by a 22.25m mast installed for our research around 1km away overlooking an Alaskan paper birch canopy (hereafter: paper birch tower).

PAM Fluorometry and Needle Physiology: We installed six Micro-PAM measuring heads (Heinz Walz GmbH, Effeltrich, Germany) on two black spruce trees located adjacent to the black spruce tower (Figure 1). Three measuring heads were installed on each tree at three heights within the canopy: low, middle, and high. These measuring heads were connected to a computer that stored data and scheduled saturation pulses. From these pulses, the standard PAM fluorescence parameters of transient fluorescence (F_t), dark-adapted minimum fluorescence (F_o), dark-adapted maximum fluorescence (F_m), and light-adapted maximum fluorescence (F_m') were measured (See Reference 13 for review). Due to the difficulties of measuring it in the field, the light-adapted minimum fluorescence (F_o') is not measured and is instead estimated from F_o, F_m, F_m' (Equation 1).[33]

$$F_o' = \frac{1}{\left(\frac{1}{F_o}\right)-\left(\frac{1}{F_m}\right)+\left(\frac{1}{F_m'}\right)} \quad (1)$$

Using these fluorescence parameters, the yields of photosystem II (Y(II)) and NPQ (Y(NPQ)) per unit quanta can be calculated (Equations 2-3).[34-35] Similarly, the maximum possible yield of photosystem II ($Y(II)_M$) can also be derived using dark-adapted fluorescence values (Equation 4).[36] These dark-adapated parameters can be used alongside F_t to continuously monitor the cumulative yield of energy release through non-regulated heat dissipation and fluorescence (Y(NO)) (Equation 5).[34] Fluorescence yield specifically can be proxied using F_t and can be estimated by assuming a maximum fluorescence yield of 10% in dark conditions and utilizing the maximum F_m value measured across the study period (F_{MR}) (Equation 6).[22]

$$Y(II) = \frac{F_m' - F_t}{F_{m'}} \quad (2)$$

$$Y(NPQ) = \frac{Ft}{F_m'} - \frac{F_t}{F_m} \quad (3)$$

$$Y(II)_M = \frac{F_m - F_O}{F_M} \quad (4)$$

$$\mathrm{Y(NO)} = \frac{F_t}{F_m} \quad (5)$$

$$Y(F) = 0.1\frac{F_o}{F_{MR}} \quad (6)$$

Phenological Remote Sensing Across Stand Types: We collected canopy-scale remote sensing measurements using the tower-based Fluospec3 system (Figure 1). Fluospec3 can be divided into three core components: the spectrometers, the camera, and the managing computer. For the spectrometers, we utilize two customized QEPro instruments (OceanInsight, Orlando, USA). The first

QEPro observes in the near-infrared wavelength range (~730-785nm) and is optimized for the retrieval of SIF. The second QEPro spans the visible and near-infrared spectrum (~400-1175nm) and is primarily used to derive vegetation indices. These spectrometers are coupled to two fiber-optic cables, one measuring downwelling irradiance and the other capturing upwelling radiance from the canopy. While the irradiance fiber is mounted on the tower, the vegetation fiber is mounted on the camera. Prior to taking spectral measurements, the camera moves to face the targeted part of the canopy, facilitating spectral measurements from different parts of the same stand. This process of moving the camera, taking, a picture, collecting spectra from both fibers, and storing the ensuing data is controlled by a Raspberry Pi 3B (Raspberry Pi Foundation, Cambridge, UK). Fluospec3 was installed near the top of both the black spruce and paper birch towers. At each site, Fluospec3 recorded spectra from six total targets every 30 minutes. All spectra were quality controlled for extreme sun zenith angles and instability in light conditions during the measurement period.

In addition to SIF, several other remote sensing parameters were used monitor plant status. The normalized difference vegetation index (NDVI), a vegetation index (VI) that responds to shifts in canopy greenness and structure, was calculated using the reflectance (ρ) from 770-780nm and 620-670nm (Equation 7).[37] This index can be used to estimate the near-infrared reflectance of vegetation (NIRv), which has been strongly correlated with plant productivity, by multiplying it by near-infrared reflectance (Equation 8).[38] The chlorophyll-carotenoid index (CCI), a VI that responds to shifts in chlorophyll and carotenoid pigments within the stand, was originally calculated using bands 1 (650nm) and 11 (530nm) from the moderate resolution imaging spectrometer (MODIS) satellite instrument.[39] Here we calculate it using the broadband reflectance from 620-670nm and from 526-536nm (Equation 9). The photochemical reflectance index (PRI), which is similarly sensitive to plant pigment status, is calculated from the reflectance at 531nm and 570nm (Equation 10).[37]

$$NDVI = \frac{\rho_{770-780} - \rho_{620-670}}{\rho_{770-780} + \rho_{620-670}} \quad (7)$$

$$NIR_V = \rho_{770-780} * NDVI \quad (8)$$

$$CCI = \frac{\rho_{526-536} - \rho_{620-670}}{\rho_{526-536} + \rho_{620-670}} \quad (9)$$

$$PRI = \frac{\rho_{531} - \rho_{570}}{\rho_{531} + \rho_{570}} \quad (10)$$

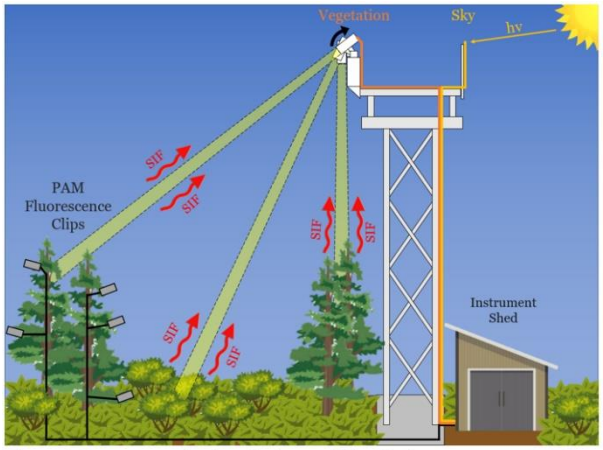

Figure 1. Instrumentation installed around the black spruce tower. PAM fluorometry measuring heads were installed at three heights (top, middle bottom) on two trees. FS3 was installed on the black spruce tower and observed the surrounding trees, including those monitored by the PAM instruments.

Results and Future Work

Needleleaf Physiology and Environmental Drivers: The partitioning of photosynthetic energy exhibited noticeably seasonal changes (Figure 2). The photosynthetic yield rose from a pre-growing season value of around 10% to around 70% during the growing season. These increases largely came at the expense of non-regulated heat dissipation, which constituted around 85% of energy usage outside of the growing season, but only around 25% during the growing season. NPQ and fluorescence yields exhibited more muted seasonal patterns in absolute terms. NPQ yield shifted upwards from 8% to 20% from April to May, but then subsided in months following June. Similarly, fluorescence yield rose from around 0.5% in March to 2% during the growing season. All yields lacked a cohesive response to changes in PAR (data not shown), but responded strongly to air temperature (Figure 3).

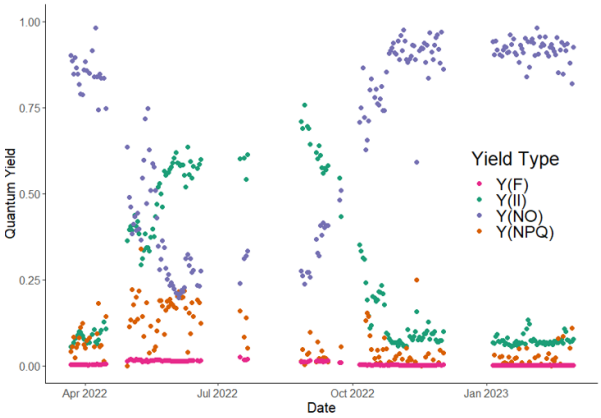

Figure 2. Seasonal variations in photosynthetic partitioning from March 2022 to March 2023. Y(F) = Quantum Yield of Fluorescence, Y(II) = Quantum Yield of Photosystem II, Y(NO) = Quantum Yield of Non-Regulated Heat Dissipation & Fluorescence, Y(NPQ) = Quantum Yield of Non-Photochemical Quenching

The strong seasonal shifts of photosynthetic partitioning reflect changes in needle strategy. During the harsh winter periods, harsh temperatures and low PAR levels prevent efficient photosynthetic activity and promote the dissipation of energy as heat. As temperature and PAR values increase, photosynthesis increasingly becomes the dominant outlet for absorbed light energy, with regulated heat dissipation via NPQ and energy loss through fluorescence also increasing. The observed shift in partitioning due to temperature supports this conclusion. The lack of change in response to PAR, meanwhile, may be due to diurnal patterns in PAR adding noise to the observed relationship at larger timescales. Future work will focus on exploring additional environmental variables, such as soil moisture, implementing improved quality control, and evaluating additional PAM-based physiology metrics.

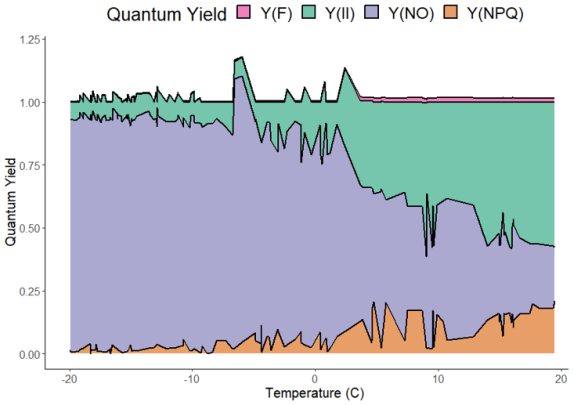

Figure 3. Temperature-driven variations in photosynthetic partitioning from March 2022 to March 2023. Y(F) = Quantum Yield of Fluorescence, Y(II) = Quantum Yield of Photosystem II, Y(NO) = Quantum Yield of Non-Regulated Heat Dissipation & Fluorescence, Y(NPQ) = Quantum Yield of Non-Photochemical Quenching.

Remotely Sensed Phenology across Stand Types: At the evergreen stand, SIF exhibited no seasonality and significant noise (Figure 4a). This stands in contrast to NDVI (4b), NIRv (4c), CCI (4d), and PRI (4e), which all exhibited clear seasonal patterns. Based on pictures from FS3's camera, snow and ice crystal melting played a significant role in driving seasonality of NDVI and PRI but did not strongly affect CCI. At the deciduous stand, all remote sensing phenometrics exhibited notable seasonality, with them suggesting a strong downregulation of photosynthesis going into the fall (Figure 5). Based on concomitant pictures taken by FS3,

all remote sensing phenometrics effectively tracked leaf senescence.

The ineffectiveness of SIF at tracking evergreen seasonality is surprising given its past successes working in these ecosystems[31] and with black spruce specifically.[21] We believe that this is the result of insufficient signal. Due to the sparse evergreen canopy, understory vegetation forms a prominent background that can confound remote sensing measurements of black spruce phenology. To mitigate this, we implemented a reduced fiber field of view (3°) at the evergreen site that allowed for measurements to be isolated to specific trees but also reduced the amount of signal being observed. While conventional vegetation indices were able to be retrieved, the comparatively small SIF signal was not. In contrast, the closed deciduous canopy allowed for a larger fiber field of view (6°) and a stronger overall signal, enabling effective SIF retrievals. Future work will focus on compromising between background effects and signal strength at this site and evaluating how different remote sensing metrics relate to different environmental parameters.

Looking across sites, NDVI and NIR_V were effective at capturing greenness and structural changes at the deciduous site but were confounded snow and ice-driven reflectance shifts at the evergreen site, making interpretation difficult. This is contrasted by CCI and, to a lesser extent, PRI, which were able to capture changes in pigments at both sites. Future work will focus on comparing these indices to environmental data and PAM physiology to better understand what aspects of phenology and physiology they respond to.

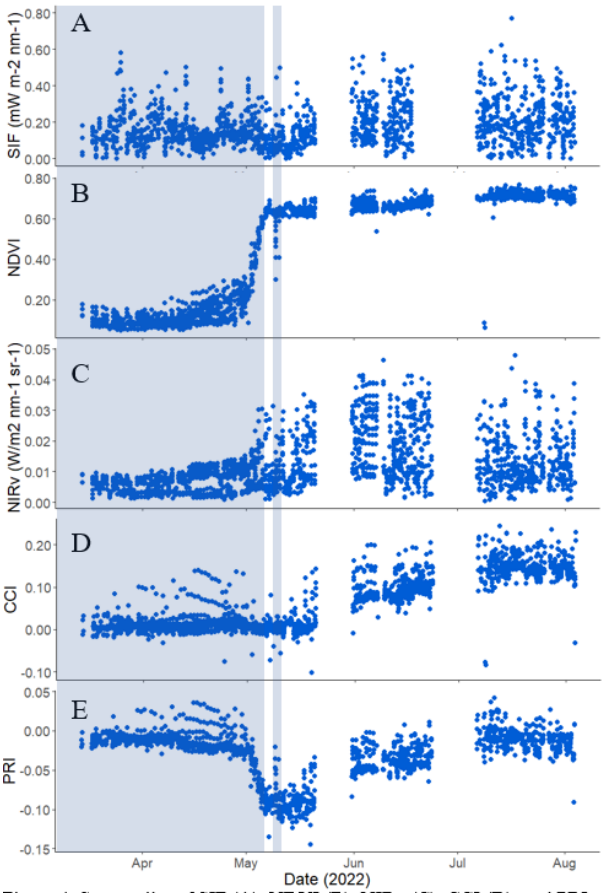

Figure 4. Seasonality of SIF (A), NDVI (B), NIRv (C), CCI (D), and PRI (E) from March to August 2022. All measurements were taken at a viewing zenith angle of 5.8° and a viewing azimuth angle of 34.9°. Blue shading denotes time periods with snow cover.

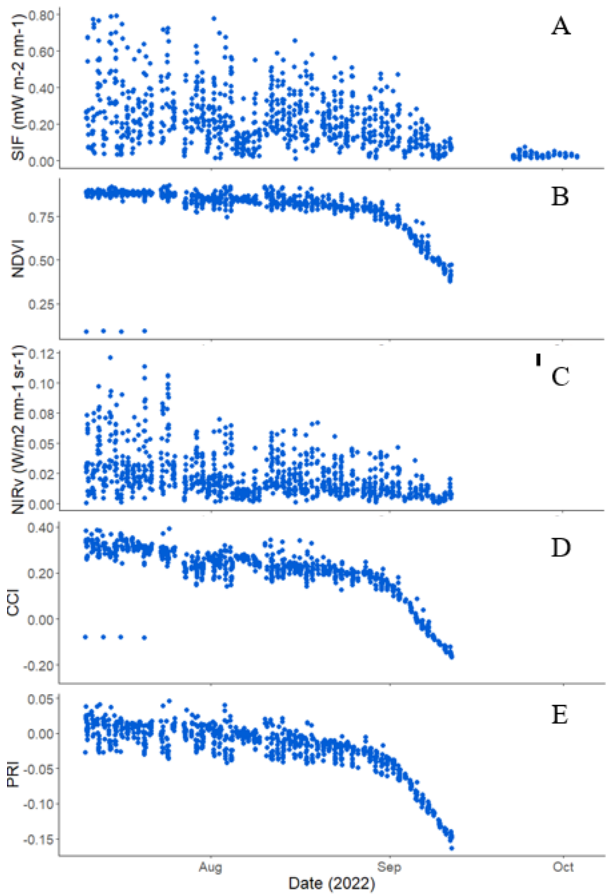

Figure 5. Seasonality of SIF (A), NDVI (B), NIRv (C), CCI (D), and PRI (E) from July to October 2022. All measurements were taken at a viewing zenith angle of 32.45° and a viewing azimuth angle of 304.23°.

Works Cited

1. Smith, D. M., Screen, J. A., Deser, C., Cohen, J., Fyfe, J. C., Garcia-Serrano, J., Jung, T., Kattsov, V., Matei, D., Msadek, R., Peings, Y., Sigmond, M., Ukita, J., Yoon, J.-H., & Zhang, X. (2019). The Polar Amplification Model Intercomparison Project (PAMIP) contribution to CMIP6: investigating the causes and consequences of polar amplification. *Geoscientific Model Development*, *12*(3), 1139–1164.

2. Gulev, S.K., P.W. Thorne, J. Ahn, F.J. Dentener, C.M. Domingues, S. Gerland, D. Gong, D.S. Kaufman, H.C. Nnamchi, J. Quaas, J.A. Rivera, S. Sathyendranath, S.L. Smith, B. Trewin, K. von Schuckmann, and R.S. Vose, 2021: Changing State of the Climate System. In *Climate Change 2021: The Physical Science Basis. Contribution of Working Group I to the Sixth Assessment Report of the Intergovernmental Panel on Climate Change*[Masson-Delmotte, V., P. Zhai, A. Pirani, S.L. Connors, C. Péan, S. Berger, N. Caud, Y. Chen, L. Goldfarb, M.I. Gomis, M. Huang, K. Leitzell, E. Lonnoy, J.B.R. Matthews, T.K. Maycock, T. Waterfield, O. Yelekçi, R. Yu, and B. Zhou (eds.)]. Cambridge University Press, Cambridge, United Kingdom and New York, NY, USA, pp. 287–422,

3. Partain, J. L., Alden, S., Strader, H., Bhatt, U. S., Bieniek, P. A., Brettschneider, B. R., ... & Ziel, R. H. (2016). An assessment of the role of anthropogenic climate change in the Alaska fire season of 2015. *Bulletin of the American Meteorological Society*, *97*(12), S14-S18

4. D'Orangeville, L., St-Laurent, M.-H., Boisvert-Marsh, L., Zhang, X., Bastille-Rousseau, G., & Itter, M. (2023). *Current Symptoms of Climate Change in Boreal Forest Trees and Wildlife BT - Boreal Forests in the Face of*

Climate Change: Sustainable Management (M. M. Girona, H. Morin, S. Gauthier, & Y. Bergeron (eds.); pp. 747–771). Springer International Publishing.

5. Hart, S. J., Henkelman, J., McLoughlin, P. D., Nielsen, S. E., Truchon-Savard, A., & Johnstone, J. F. (2019). Examining forest resilience to changing fire frequency in a fire-prone region of boreal forest. *Global Change Biology*, *25*(3), 869–884.

6. Zhao, B., Zhuang, Q., Shurpali, N., Köster, K., Berninger, F., & Pumpanen, J. (2021). North American boreal forests are a large carbon source due to wildfires from 1986 to 2016. *Scientific Reports*, *11*(1), 7723

7. Walker, X. J., Baltzer, J. L., Cumming, S. G., Day, N. J., Ebert, C., Goetz, S., Johnstone, J. F., Potter, S., Rogers, B. M., Schuur, E. A. G., Turetsky, M. R., & Mack, M. C. (2019). Increasing wildfires threaten historic carbon sink of boreal forest soils. *Nature*, *572*(7770), 520–523.

8. Reich, P. B., Sendall, K. M., Stefanski, A., Wei, X., Rich, R. L., & Montgomery, R. A. (2016). Boreal and temperate trees show strong acclimation of respiration to warming. *Nature*, *531*(7596), 633–636.

9. Allison, S. D., & Treseder, K. K. (2011). Climate change feedbacks to microbial decomposition in boreal soils. *Fungal Ecology*, *4*(6), 362–374. https://doi.org/https://doi.org/10.1016/j.funeco.2011.01.003

10. Farquhar, G. D., Von Caemmerer, S., & Berry, J. A. (1980). A Biochemical Model of Photosynthetic CO 2 Assimilation in Leaves of C 3 Species. In *Planta* (Vol. 149).

11. Dusenge, M. E., Ward, E. J., Warren, J. M., Stinziano, J. R., Wullschleger, S. D., Hanson, P. J., & Way, D. A. (2021). Warming induces divergent stomatal dynamics in co-occurring boreal trees. *Global Change Biology*, *27*(13), 3079–3094.

12. Zadworny, M., Mucha, J., Bagniewska-Zadworna, A., Żytkowiak, R., Mąderek, E., Danusevičius, D., Oleksyn, J., Wyka, T. P., & McCormack, M. L. (2021). Higher biomass partitioning to absorptive roots improves needle nutrition but does not alleviate stomatal limitation of northern Scots pine. *Global Change Biology*, *27*(16), 3859–3869.

13. Baker, N. R. (2008). Chlorophyll fluorescence: A probe of photosynthesis in vivo. In *Annual Review of Plant Biology* (Vol. 59, pp. 89–113).

14. Johnstone, J. F., Hollingsworth, T. N., Chapin Iii, F. S., & Mack, M. C. (2010). Changes In Fire Regime break the legacy lock on successional trajectories in Alaskan boreal forest. *Global Change Biology*, *16*(4), 1281–1295.

15. Mack, M. C., Walker, X. J., Johnstone, J. F., Alexander, H. D., Melvin, A. M., Jean, M., & Miller, S. N. (2021).

Carbon loss from boreal forest wildfires offset by increased dominance of deciduous trees.

16. Gu, H., Qiao, Y., Xi, Z., Rossi, S., Smith, N. G., Liu, J., & Chen, L. (2022). Warming-induced increase in carbon uptake is linked to earlier spring phenology in temperate and boreal forests. *Nature Communications*, *13*(1), 3698.

17. Hynes, A., & Hamann, A. (2020). Moisture deficits limit growth of white spruce in the west-central boreal forest of North America. *Forest Ecology and Management*, *461*, 117944.

18. Stinziano, J. R., & Way, D. A. (2014). Combined effects of rising [CO2] and temperature on boreal forests: growth, physiology and limitations. *Botany*, *92*(6), 425–436.

19. Ruban, A. V. (2016). Nonphotochemical Chlorophyll Fluorescence Quenching: Mechanism and Effectiveness in Protecting Plants from Photodamage. *Plant Physiology*, *170*(4), 1903–1916.

20. Meroni, M., & Colombo, R. (2006). Leaf level detection of solar induced chlorophyll fluorescence by means of a subnanometer resolution spectroradiometer. *Remote Sensing of Environment*, *103*(4), 438–448.

21. Raczka, B., Porcar-Castell, A., Magney, T., Lee, J. E., Köhler, P., Frankenberg, C., Grossmann, K., Logan, B. A., Stutz, J., Blanken, P. D., Burns, S. P., Duarte, H., Yang, X., Lin, J. C., & Bowling, D. R. (2019). Sustained Nonphotochemical Quenching Shapes the Seasonal Pattern of Solar-Induced Fluorescence at a High-Elevation Evergreen Forest. *Journal of Geophysical Research: Biogeosciences*, *124*(7), 2005–2020.

22. Porcar-Castell, A. (2011). A high-resolution portrait of the annual dynamics of photochemical and non-photochemical quenching in needles of Pinus sylvestris. *Physiologia Plantarum*, *143*(2), 139–153.

23. Verbyla, D. (2008). The greening and browning of Alaska based on 1982–2003 satellite data. *Global Ecology and Biogeography*, *17*(4), 547–555.

24. Keenan, T. F., & Riley, W. J. (2018). Greening of the land surface in the world's cold regions consistent with recent warming. *Nature Climate Change*, *8*(9), 825–828.

25. Park, T., Ganguly, S., Tømmervik, H., Euskirchen, E. S., Høgda, K.-A., Karlsen, S. R., Brovkin, V., Nemani, R. R., & Myneni, R. B. (2016). Changes in growing season duration and productivity of northern vegetation inferred from long-term remote sensing data. *Environmental Research Letters*, *11*(8), 84001.

26. Walther, S., Voigt, M., Thum, T., Gonsamo, A., Zhang, Y., Köhler, P., Jung, M., Varlagin, A., & Guanter, L. (2016). Satellite chlorophyll fluorescence measurements reveal large-scale decoupling of photosynthesis and greenness dynamics in boreal evergreen forests. *Global Change Biology*, *22*(9), 2979–2996.

27. Huang, K., Zhang, Y., Tagesson, T., Brandt, M., Wang, L., Chen, N., Zu, J., Jin, H., Cai, Z., Tong, X., Cong, N., & Fensholt, R. (2021). The confounding effect of snow cover on assessing spring phenology from space: A new look at trends on the Tibetan Plateau. *Science of The Total Environment*, *756*, 144011.

28. Frankenberg, C., & Berry, J. (2017). Solar induced chlorophyll fluorescence: Origins, relation to photosynthesis and retrieval. In *Comprehensive Remote Sensing* (Vols. 1–9, pp. 143–162). Elsevier.

29. Ni, Z., Lu, Q., Huo, H., & Zhang, H. (2019). Estimation of chlorophyll fluorescence at different scales: A review. In *Sensors (Switzerland)* (Vol. 19, Issue 13). MDPI AG.

30. Li, X., Xiao, J., He, B., Altaf Arain, M., Beringer, J., Desai, A. R., Emmel, C., Hollinger, D. Y., Krasnova, A., Mammarella, I., Noe, S. M., Ortiz, P. S., Rey-Sanchez, A. C., Rocha, A. V., & Varlagin, A. (2018). Solar-induced chlorophyll fluorescence is strongly correlated with terrestrial photosynthesis for a wide variety of biomes: First global analysis based on OCO-2 and flux tower observations. *Global Change Biology*, *24*(9), 3990–4008.

31. Pierrat, Z., Nehemy, M. F., Roy, A., Magney, T., Parazoo, N. C., Laroque, C., Pappas, C., Sonnentag, O., Grossmann, K., Bowling, D. R., Seibt, U., Ramirez, A., Johnson, B., Helgason, W., Barr, A., & Stutz, J. (2021). Tower-Based Remote Sensing Reveals Mechanisms Behind a Two-phased Spring Transition in a Mixed-Species Boreal Forest. *Journal of Geophysical Research: Biogeosciences*, *126*(5), e2020JG006191.

32. National Ecology Observatory Network. (n.d.). *Caribou-Poker Creeks Research Watershed / BONA*. National Ecology Observatory Network. Retrieved March 30, 2023, from https://www.neonscience.org/field-sites/bona

33. Oxborough, K., & Baker, N. R. (1997). Resolving chlorophyll a fluorescence images of photosynthetic efficiency into photochemical and non-photochemical components – calculation of qP and Fv-/Fm-; without measuring Fo-; *Photosynthesis Research*, *54*(2), 135–142.

34. Genty, B., Briantais, J. M., & Baker, N. R. (1989). The relationship between the quantum yield of photosynthetic electron transport and quenching of chlorophyll fluorescence. *Biochimica et Biophysica Acta - General Subjects*, *990*(1), 87–92.

35. Genty B, Harbinson J, Cailly AL and Rizza F (1996) Fate of excitation at PS II in leaves: the non-photochemical side. Presented at: The Third BBSRC Robert Hill Symposium on Photosynthesis, March 31 to April 3, 1996, University of Sheffield, Department of Molecular Biology and Biotechnology, Western Bank, Sheffield, UK, Abstract P28

36. Kitajima, M., & Butler, W. L. (1975). QUENCHING OF CHLOROPHYLL FLUORESCENCE AND PRIMARY PHOTOCHEMISTRY IN CHLOROPLASTS BY DIBROMOTHYMOQUINONE. In *Biochimica et Biophysica Acta* (Vol. 376).

37. Xue, J., & Su, B. (2017). Significant Remote Sensing Vegetation Indices: A Review of Developments and Applications. *Journal of Sensors*, *2017*, 1353691. https://doi.org/10.1155/2017/1353691

38. Badgley, G., Field, C. B., & Berry, J. A. (2017). Canopy near-infrared reflectance and terrestrial photosynthesis. *Science Advances*, *3*(3), e1602244.

39. Gamon, J. A., Huemmrich, K. F., Wong, C. Y. S., Ensminger, I., Garrity, S., Hollinger, D. Y., Noormets, A., & Peñuelas, J. (2016). A remotely sensed pigment index reveals photosynthetic phenology in evergreen conifers. *Proceedings of the National Academy of Sciences*, *113*(46), 13087–13092.